Complex networks embedded in space: Dimension and scaling relations between mass, topological distance, and Euclidean distance

Thorsten Emmerich,[1] Armin Bunde,[1] Shlomo Havlin,[2] Guanliang Li,[3] and Daqing Li[4]
[1]*Institut für Theoretische Physik, Justus-Liebig-Universität Giessen, 35392 Giessen, Germany*
[2]*Department of Physics, Bar-Ilan University, Ramat-Gan 52900, Israel*
[3]*Center for Polymer Studies, Department of Physics, Boston University, Boston, Massachusetts 02215, USA*
[4]*School of Reliability and Systems Engineering, Beihang University, Beijing 100191, China*
(Received 8 October 2012; revised manuscript received 31 January 2013; published 6 March 2013)

Many real networks are embedded in space, and often the distribution of the link lengths r follows a power law, $p(r) \sim r^{-\delta}$. Indications that such systems can be characterized by the concept of dimension were found recently. Here, we present further support for this claim, based on extensive numerical simulations of model networks with a narrow degree distribution, embedded in lattices of dimensions $d_e = 1$ and $d_e = 2$. For networks with $\delta < d_e$, d is infinity, while for $\delta > 2d_e$, d has the value of the embedding dimension d_e. In the intermediate regime of interest $d_e \leqslant \delta < 2d_e$, our numerical results suggest that d decreases continuously from $d = \infty$ to d_e, with $d - d_e \propto (2 - \delta')/[\delta'(\delta' - 1)]$ and $\delta' = \delta/d_e$. We also analyze how the mass M and the Euclidean distance r increase with the topological distance ℓ (minimum number of links between two sites in the network). Our results suggest that in the intermediate regime $d_e \leqslant \delta < 2d_e$, $M(\ell)$ and $r(\ell)$ increase with ℓ as a *stretched* exponential, $M(\ell) \sim \exp[Ad\ell^{\delta'(2-\delta')}]$ and $r(\ell) \sim \exp[A\ell^{\delta'(2-\delta')}]$, such that $M(\ell) \sim r(\ell)^d$. For $\delta < d_e$, M increases exponentially with ℓ (as known for $\delta = 0$), while r is constant and independent of ℓ. For $\delta \geqslant 2d_e$, we find the expected power-law scaling, $M(\ell) \sim \ell^{d_\ell}$ and $r(\ell) \sim \ell^{1/d_{\min}}$, with $d_\ell d_{\min} = d$. In $d_e = 1$, we find the expected result, $d_\ell = d_{\min} = 1$, while in $d_e = 2$ we find surprisingly that although $d = 2$, $d_\ell > 2$ and $d_{\min} < 1$, in contrast to regular lattices.

DOI: 10.1103/PhysRevE.87.032802 PACS number(s): 89.75.Da, 05.10.Ln

I. INTRODUCTION

It has been realized in the last decades that a large number of complex systems are structured in the form of networks. The structures can be manmade such as the World Wide Web and transportation or power grid networks or natural such as protein and neural networks [1–19]. When studying the properties of these networks it is usually assumed that spatial constraints can be neglected. This assumption is certainly correct for networks such as the World Wide Web (WWW) or the citation network where the real (Euclidean) distance does not play any role, but it may not be justified in networks where the Euclidean distance matters [20]. Typical examples of such networks include the Internet [2,8], airline networks [21,22], wireless communication networks [23], and social networks (like friendship and author networks) [24,25], which are all embedded in two-dimensional space (surface of the earth), as well as protein and neural networks [26], which are embedded in three dimensions.

To model these networks, two network classes are of particular interest: Erdös-Rényi (ER) graphs [27,28] and Barabasi-Albert (BA) scale free networks [29]. In ER networks, the distribution of the number k of links per node (degree distribution) is Poissonian with a pronounced maximum at a certain k value, such that nearly each node is linked to the same number of nodes. In BA networks, the distribution follows a power law $P(k) \sim k^{-\alpha}$, with α typically between 2 and 3. Here we do not study BA networks but focus solely on ER-type networks embedded in one- and two-dimensional space. We actually use a degree distribution that is close to a delta function (as the case in simple lattices). We found that the results are the same for both kinds of distributions. We follow Refs. [30–32] and assume that nodes are connected to each other with a probability $p(r) \sim r^{-\delta}$, where r is the Euclidean distance between the nodes. The choice of a power law for the distance distribution is supported from findings in the Internet, airline networks, human travel networks, and other social networks [22,25,33]. Our model of embedding links of length r, chosen from Eq. (1), in a d_e- dimensional lattice, can be regarded as a generalization of the known Watts-Strogatz model [3,4] and the Kleinberg model [34]. In both models, long-range links are added in a lattice system. In the Watts-Strogatz model these links are chosen with the same probability, while in the Kleinberg model the link lengths are chosen from a power-law distribution $p(r) \sim r^{-\delta}$ as in the case considered here. Other methods for embedding networks in Euclidean space have been proposed in [35–38].

It has recently been shown that spatial constraints are important and may alter the dimension of the network (obtained from the scaling relation between mass M and Euclidean distance r, $M \sim r^d$) and its other topological properties (such as the dependence of the mean topological distance on the system size) as well as their robustness [30,31]. Here we are interested in studying how in these model networks the spatial constraints quantified by the distance exponent δ modify the scaling relations between mass (number of nodes), Euclidean distance r, and topological distance ℓ. Our earlier study on ER networks embedded in a square lattice (with dimension $d_e = 2$) indicates that by varying the exponent δ one can actually change continuously the dimension d of the network, from $d = \infty$ for $\delta < 2$ to $d = 2$ for $\delta > 4$ [32]. In the present paper we present further extensive numerical simulations for $d_e = 2$ that support this claim as well as simulations in linear chains ($d_e = 1$) that suggest analogous conclusions. In $d_e = 1$ we find that for $\delta < 1$ the system behaves like an infinite-dimensional

network (as the original ER network). When continuously increasing δ the dimension becomes finite for $\delta > 1$ and approaches $d = 1$ for $\delta > 2$. Since the dimension of a system plays a critical role in many physical phenomena such as diffusion, percolation, and phase transition phenomena, our results are important for understanding and characterizing the properties of real world networks.

Our paper is organized as follows. In Sec. II, we discuss the characteristic distances in the spatially constrained networks. In Sec. III we describe the method to generate the spatial network models. In Sec. IV we present our numerical results for the dimension d, for networks embedded in linear chains and in square lattices, that we obtain from the scaling relation of the mass M and the distance r. In Sec. V we present our numerical results for the dimension d, that we obtain from the scaling relation of the probability of return to the origin P_0 of a diffusing particle and its distance r. In Sec. VI, we discuss the scaling of the mass M and the Euclidean distance r with the topological distance ℓ. The conclusions in Sec. VII summarize our main results.

II. CHARACTERISTIC DISTANCES

First we estimate how the characteristic distances, in a network of L^{d_e} nodes, depend on its linear size L, on δ, and on the embedding dimension d_e. We normalize the distance distribution $p(r)$ such that $\int_1^L dr\, r^{d_e-1} p(r) = 1$, which yields

$$p(r) = \begin{cases} (d_e - \delta) L^{-(d_e-\delta)} r^{-\delta} , & \delta < d_e, \\ (\delta - d_e) r^{-\delta} , & \delta > d_e. \end{cases} \quad (1)$$

From $p(r)$ we obtain $\overline{r^n} = \int_1^L dr\, r^{d_e-1} r^n\, p(r)$ and the related length scales $\bar{r}_n \equiv (\overline{r^n})^{1/n}$. The maximum distance $r_{\max}$ is determined by $L^{d_e} \int_{r_{\max}}^L dr\, r^{d_e-1} p(r) \simeq 1$. The results for $\overline{r^n}$ and $r_{\max}$ are

$$\overline{r^n} = \begin{cases} \frac{d_e-\delta}{d_e+n-\delta} L^n , & \delta < d_e, \\ L^n/\ln(L) , & \delta = d_e, \\ \frac{\delta-d_e}{d_e+n-\delta} L^{d_e+n-\delta} , & d_e < \delta < d_e + n, \\ n \ln(L) , & \delta = d_e + n, \\ \frac{d_e-\delta}{d_e+n-\delta} , & \delta > d_e + n, \end{cases} \quad (2)$$

and

$$r_{\max} \simeq \begin{cases} L , & \delta < 2d_e, \\ L^{d_e/(\delta-d_e)} , & \delta \geqslant 2d_e. \end{cases} \quad (3)$$

Accordingly, for $\delta < d_e$ all length scales ($\bar{r}_n$ and $r_{\max}$) are proportional to L, the spatial constraints are irrelevant, and the system can be regarded as an infinite-dimensional system. On the other hand, for $\delta > 2d_e$, $\bar{r}_n/L$ and $r_{\max}/L$ tend to zero in the asymptotic limit. In this case, we expect that the physical properties of the network are close to those of regular lattices of dimension d_e. However, large finite-size effects are expected for δ close to $2d_e$ where $r_{\max}/L$ decays only very slowly to zero. In the intermediate δ regime $d_e \leqslant \delta < 2d_e$, $r_{\max}$ scales as L, while $\bar{r}_n/L$ tends to zero in the asymptotic limit. In this regime our simulation results (Sec. IV) suggest intermediate behavior represented by a dimension between d_e and infinity that changes with δ.

III. GENERATION OF THE NETWORKS

The nodes of the network are located at the sites of a d_e-dimensional regular lattice, in our case a linear chain of length L ($d_e = 1$) or a square lattice of size $L \times L$ ($d_e = 2$). We assign to each node a fixed number k of links (in most cases, $k = 4$). Actually this network is a random regular network since all nodes have the same degree. It is expected (and we have also verified it numerically) that ER networks and random regular networks (with the same spatial constraints) are in the same universality class.

To generate the spatially embedded networks, we use the following iterative algorithm: (i) We pick a node i randomly and choose, for one of its available k_i links, a distance r ($1 \leqslant r \leqslant L$) from the given probability distribution $p(r)$, Eq. (1). It is easy to see that the distance r can be obtained from random numbers $0 < u \leqslant 1$ chosen from the uniform distribution, by

$$r = \begin{cases} [1 - u(1 - L^{d_e-\delta})]^{1/(d_e-\delta)} , & \delta \neq d_e, \\ L^u , & \delta = d_e. \end{cases} \quad (4)$$

(ii) We consider all N_r nodes between distance $r - \Delta r$ and r from node i, that are not yet connected to node i. Without loss of generality, we choose $\Delta r = 1$ for the linear chain and $\Delta r = 0.4$ for the square lattice. These choices of Δr ensure that the desired distribution function $p(r) \propto r^{-\delta}$ is fulfilled in the whole range of r except at r values close to the system size (see Fig. 2). (iii) We pick randomly one of these nodes j. If node j has at least one available link, we connect it with node i. If not, we do not connect it. Then we return to (i) and proceed with another randomly chosen node. At each step of the process, either 2 or zero links are added. For generating the network, we have typically performed $10L^{d_e}$ trials. We found that the results remained stable when the number of trials was further enhanced (up to $10^3 L^{d_e}$ trials). Due to the generation process, the nodes of the final network do not all have exactly the same degree, but the degree follows a narrow distribution with a mean $\bar{k}$ slightly below $k = 4$. Figure 1

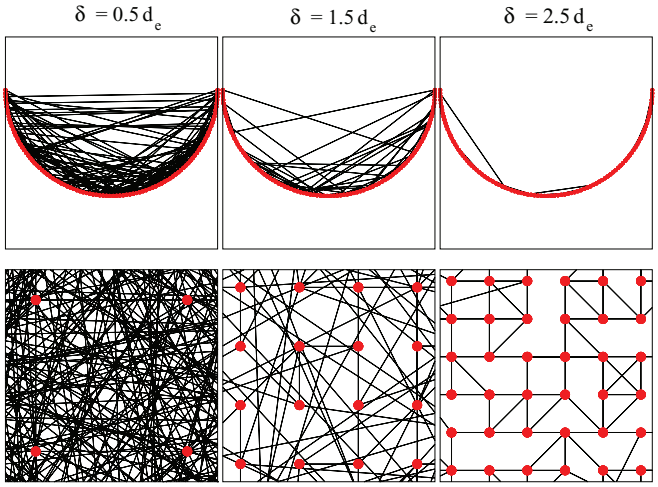

FIG. 1. (Color online) Illustration of ER networks embedded in linear chains (top) and square lattices (bottom), for various distance exponents δ. For transparency, the linear chains are shown as semicircles.

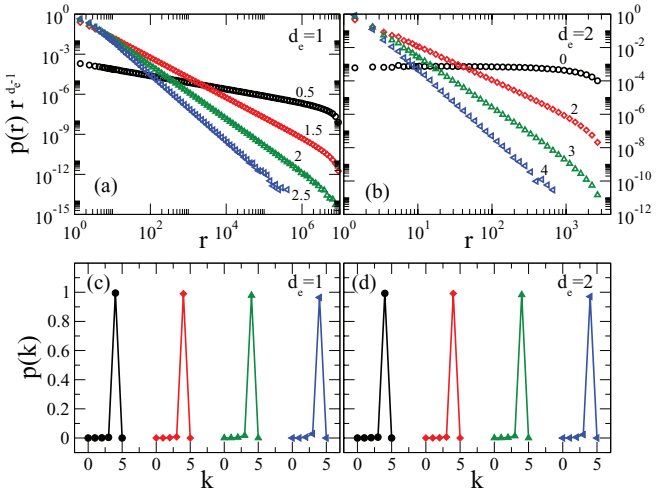

FIG. 2. (Color online) The distance distribution $p(r)\,r^{d_e-1}$ for ER networks embedded (a) in linear chains where $d_e = 1$ and (b) in square lattices where $d_e = 2$, when $\delta = 0.5d_e$ (black circle), $1.5d_e$ (red diamond), $2d_e$ (green triangle up), $2.5d_e$ (blue triangle left), and $k = 4$. The numbers denote the slopes of $P(r)r^{d_e-1}$, which are identical to the anticipated ones. For the same set of parameters as in (a) and (b), panels (c) and (d) show the degree distribution $p(k)$, which is $\cong 1$ for $k = 4$ and $\cong 0$ otherwise.

illustrates the ER networks embedded in $d_e = 1$ and $d_e = 2$ for $\delta = 0.5d_e$, $1.5d_e$, and $2.5d_e$. Figure 2 shows the actual narrow degree distribution as well as $p(r)$ obtained in the simulations.

IV. THE DIMENSION OF THE NETWORKS

For determining the dimensions of the spatially embedded networks, we follow the method developed by Li *et al.* [32]. A similar technique has been used before in disordered systems to calculate the fractal dimension, e.g., [39]. We use the fact that the mass M (number of nodes) of an object within a hypersphere of radius r scales with r as

$$M \sim r^d, \tag{5}$$

where the exponent d represents the dimension of the network. When using this relation without taking into account the way the nodes are linked, one trivially and erroneously finds that the dimension of the network is identical to the dimension d_e of the embedding space.

To properly take into account the connectivity, when considering the dimension of the network, we proceed as follows (see Fig. 3): We choose a node as origin and determine its nearest neighbors (referred to as shell $\ell = 1$) and their number $S(1)$, the number of second nearest neighbors $S(2)$ in shell $\ell = 2$, and so on. Next we measure the mean Euclidean distance $r(\ell)$ of the nodes in shell ℓ from the origin and determine the number of nodes $M(\ell) = \sum_{i=1}^{\ell} S(i)$ within shell ℓ. To improve the statistics, we repeat the calculations for many origin nodes and then average $r(\ell)$ and $M(\ell)$. To reduce boundary effects, we do not choose the origin nodes randomly in the underlying lattice, but from a region with radius $L/10$ around the central node. From the scaling relation between

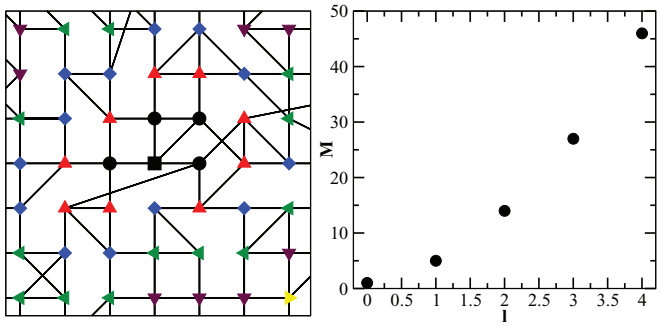

FIG. 3. (Color online) Illustration of the shells $S(0)$ (black square), $S(1)$ (black circle), $S(2)$ (red triangle up), $S(3)$ (blue diamond), $S(4)$ (green triangle left), $S(5)$ (brown triangle down), and $S(6)$ (yellow triangle right) for ER networks embedded in a square lattice with $k = 4$ (left panel), and the mass M as function of l within these shells (right panel).

the average M and the average r, Eq. (5), we determine the dimension d of the network.

Figure 4 shows the results for networks embedded in linear chains, for distance exponents δ between 0.5 d_e and $2.5d_e$. In (a), we consider networks with $k = 4$ fixed and different system sizes ($N = 10^5$, 10^6, and 10^7), while in (b) we consider networks with a fixed size $N = 10^7$ and various k values ($k =$ 3,4,6). In both panels, we have plotted M as a function of $r/\bar{r}$, where $\bar{r} \equiv \bar{r}_1$ is the mean length of the links in the network; see Eq. (2).

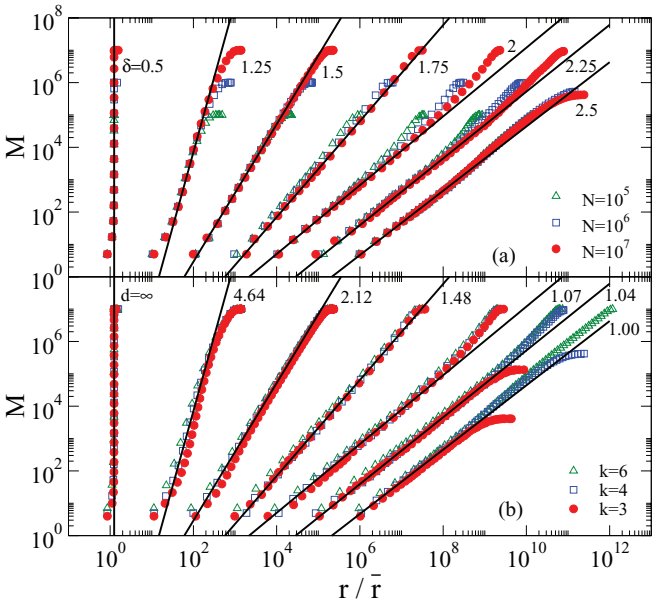

FIG. 4. (Color online) (a) The mass M as function of the relative distance $r/\bar{r}$ for ER networks embedded in linear chains with $k = 4$, for the system sizes $N = 10^5$, 10^6, and 10^7 with $\delta =$ 0.5, 1.25, 1.5, 1.75, 2, 2.25, 2.5 (from left to right). The straight lines are best fits to the data that yield the dimension d of the network. (b) The same as panel (a), but for $N = 10^7$ and $k = 3$,4, and 6. The straight lines in both panels are identical. The slopes yield the dimensions of the embedded networks $\delta =$ ∞, 4.64, 2.12, 1.48, 1.07, 1.04, and 1.00 (from left to right).

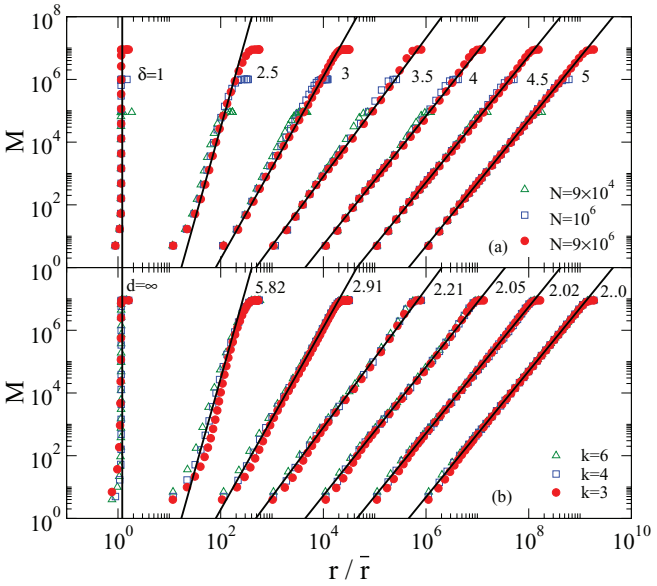

FIG. 5. (Color online) The same as Fig. 4, but for ER networks embedded in a square lattice, the system sizes are $N = 9 \times 10^4$, 10^6, and 9×10^6 with $\delta = 1$, 2.5, 3, 3.5, 4, 4.5, 5 (from left to right). The straight lines in both panels are identical. The slopes yield the dimensions of the embedded networks $\delta = \infty$, 5.82, 2.91, 2.21, 2.05, 2.02, and 2.00 (from left to right).

Figure 4(a) shows that for δ in the interesting regime between d_e and $2d_e$, the curves for different N collapse nicely [for transparency, the curves (except $\delta = 0.5$) have been shifted along the x axis by a factor of 10, 10^2, 10^3, 10^4, and 10^5]. From the slopes of the straight lines, we obtain the dimensions $d = \infty$ ($\delta = 0.5$), $d \cong 4.64$ ($\delta = 1.25$), $d \cong 2.12$ ($\delta = 1.5$), and $d \cong 1.48$ ($\delta = 1.75$). For $\delta \geqslant 2$, the data start to overshoot above some crossover value that increases with the system size and thus can be regarded as a finite-size effect. To understand the reason for this crossover note that a node close to the boundary has a considerably higher probability to be linked with nodes closer to the center of the underlying lattice. As a consequence, for large shell numbers ℓ, the mean Euclidean distance of the nodes from the origin node will be underestimated and thus the mass within large Euclidean distances overestimated. This effect is most pronounced in the linear chain, for intermediate δ values, and gives rise to the overshooting of $M(r)$ for δ between 2 and 2.5, where $d \simeq d_e$. For $\delta = 2.5$ and $N = 10^7$, the total number of nodes in the spatially constrained network is well below N, since the network is separated into smaller clusters. For larger k values, this effect is less likely to appear. Figure 4(b) shows that the dimension of the networks does not depend on their average degree. The $M(r)$ curves collapse for different k, and thus give rise to the same dimensions. This indicates the universality feature of the dimension.

Figure 5 shows the corresponding results for networks embedded in square lattices ($d_e = 2$), again for 7 exponents δ between $0.5d_e$ and $2.5d_e$, three network sizes ($N = 9 \times 10^4, 10^6$, and 9×10^6), and three k values ($k = 3,4,6$). From the slopes of the straight lines we obtain $d = \infty$ ($\delta = 1$), $d \cong 5.82$ ($\delta = 2.5$), $d \cong 2.91$ ($\delta = 3$), and $d \cong 2.21$ ($\delta = 3.5$). For δ above 4, d is close to d_e, as expected. The figure confirms

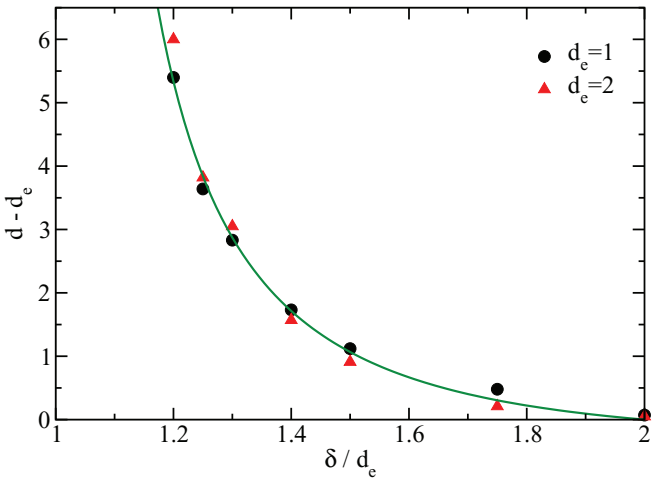

FIG. 6. (Color online) The difference between network dimension d and embedding dimension d_e as a function of δ/d_e for $d_e = 1$ (black circles) and $d_e = 2$ (red triangles). For $\delta/d_e < 1$, $d - d_e = \infty$.

that the finite-size effects in $d_e = 2$ are considerably less pronounced than in $d_e = 1$, contrary to the intuition, since the linear size of the underlying embedding lattice is considerably higher in $d_e = 1$ than in $d_e = 2$. As in $d_e = 1$, the dimensions are independent of the mean degree of the networks.

Figure 6 summarizes our results for the dimensions of the spatially embedded networks in the intermediate δ regime between d_e and $2d_e$, where the dimension is supposed to bridge the gap between $d = \infty$ for the unconstrained case δ below d_e and $d = d_e$ for the highly constrained case δ above $2d_e$. The figure shows $d - d_e$ as a function of the relative distance exponent $\delta' = \delta/d_e$ for both considered lattices. The figure shows that in both cases, the curves approximately collapse to a single line which can be represented by

$$d - d_e = c\frac{2 - \delta'}{\delta'(\delta' - 1)}, \quad 1 < \delta' < 2, \tag{6}$$

where $c \cong 1.60$. According to Eq. (6), $d - d_e$ diverges for δ' approaching the critical relative distance exponent $\delta' = 1$. The simplicity of Eq. (6) suggests that it might be derived analytically. However, we were unable to find an analytical solution. We would like to mention that it is generally difficult to obtain analytical results for (fractal) dimensions of irregular systems. An exception is the fractal dimension d of the percolation cluster in $d_e = 2$ and $d_e \geqslant 6$, but for $2 < d_e < 6$ no useful analytical description is known.

V. THE PROBABILITY OF RETURN TO THE ORIGIN

The network dimension plays an important role also in physical processes such as diffusion [40–42]. The probability $P_0(t)$ that a diffusing particle, after having traveled t steps, has returned to the origin is related to the root-mean-square displacement $r(t)$ of the particle by [32,42,43]

$$P_0(t) \sim r(t)^{-d}. \tag{7}$$

To derive Eq. (7) one assumes that the probability of the particle to be in any site in the volume $V(t) = [r(t)]^d$ is the same. As a consequence, $P_0(t) \sim 1/V(t)$, which leads to Eq. (7). Figure 7 shows P_0 as a function of $r/\bar{r}$ in $d_e = 1$ and

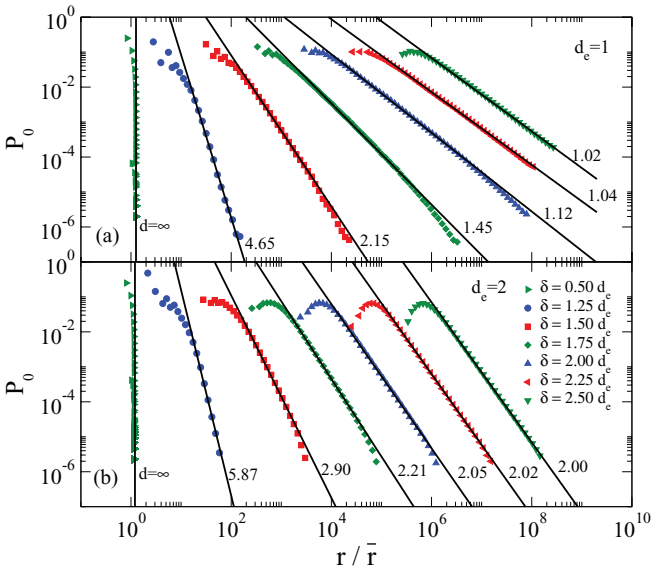

FIG. 7. (Color online) (a) The probability P_0 that a diffusing particle is at its starting site, after traveling an average distance r, as a function of the relative distance $r/\bar{r}$ for ER networks embedded in linear chains with $k = 4$, for the system size $N = 10^7$ with $\delta = 0.5, 1.25, 1.5, 1.75, 2, 2.25, 2.5$ (from left to right). The straight lines are best fits to the data that yield the dimension d of the network. (b) The same as panel (a), but for ER networks embedded in a square lattice, the system size is $N = 9 \times 10^6$ with $\delta = 1, 2.5, 3, 3.5, 4, 4.5, 5$ (from left to right). Note that the values of d obtained here are almost the same as those obtained by direct measurements in Figs. 4 and 5.

2, for the same δ values as in Figs. 4 and 5. For convenience, we show only the results for the largest system size, $N = 10^7$ for $d_e = 1$ and $N = 9 \times 10^6$ for $d_e = 2$. To obtain $P_0(t)$, we averaged, for each value of δ, over 10^4 diffusing particles and 50 network realizations. From the straight lines in the double-logarithmic presentations of Fig. 7 we obtain the dimension of the networks, which are listed in the figure. The dimensions obtained in Fig. 7 agree very well with those obtained by the direct measurements in Figs. 4 and 5.

VI. THE TOPOLOGICAL DIMENSION AND THE DIMENSION OF THE SHORTEST PATH

In order to find how M scales with the Euclidean distance r, we determined in Sec. IV how M and r scale with the topological length ℓ, and obtained the dimension d from $M(\ell) \sim r(\ell)^d$. In this section, we discuss explicitly how M and r depend on ℓ.

It is well known that for regular lattices as well as for fractal structures, M and r scale with ℓ as power laws,

$$M(\ell) \sim \ell^{d_\ell}, \tag{8a}$$

$$r(\ell) \sim \ell^{1/d_{\min}}, \tag{8b}$$

where d_ℓ is the topological ("chemical") dimension and $d_{\min}$ is the dimension of the shortest path; see, e.g., [39,44]. For regular lattices of dimension d_e, $d_\ell = d_e$ and $d_{\min} = 1$. Thus we expect that for $\delta \geqslant 2d_e$, the power-law relations (VI) hold.

For $\delta = 0$ the network has no spatial constraints and it is known that the mean topological distance $\langle \ell \rangle$ between 2 nodes on the network scales with the network size N as $\langle \ell \rangle \sim \log_{10} N$ [10]. This represents the small world nature of random graphs. Since N plays the role of the mass M of the network, it follows that M increases exponentially with ℓ; i.e., $M(\ell) \sim \exp(A\ell)$. We expect that this relation holds for $\delta < d_e$ where $r_{\max}$ and $r/\bar{r}$ are both proportional to the linear scale L of the network; see Eqs. (2) and (3). Since for $\delta > 2d_e$ we expect power-law relations (8), we conjecture that in the intermediate regime $d_e \leqslant \delta < 2d_e$, $M(\ell)$ will increase slower than exponential and faster than a power law, via a stretched exponential,

$$M(\ell) \sim \exp(A\ell^\alpha), \quad d_e \leqslant \delta < 2d_e. \tag{9}$$

This function can bridge between the exponential behavior for $\delta < d_e$ and the power law for $\delta > 2d_e$. For δ approaching d_e from above, α should approach 1, while for δ approaching $2d_e$ from below, α should approach 0, consistent with a power law. The conjecture Eq. (9) is supported by earlier numerical simulations [30] where it was found that in the intermediate regime, ℓ scales as $(\log_{10} N)^\beta$, leading to $\alpha = 1/\beta$. On the basis of numerical simulations it was estimated [30] that $\alpha \simeq \delta(2-\delta)$ in $d_e = 1$ and $\alpha \simeq \delta(4-\delta)/4$ in $d_e = 2$, which actually can be combined into a single equation, $\alpha = \delta'(2-\delta')$, when the relative distance exponent $\delta' = \delta/d_e$ is introduced. Thus our conjecture (9) becomes

$$M(\ell) \sim \begin{cases} e^{A\ell} & , \quad \delta' < 1, \\ e^{A\ell^{\delta'(2-\delta')}} & , \quad 1 \leqslant \delta' < 2, \end{cases} \tag{10}$$

where the prefactor A may depend on δ' and d_e. To test this hypothesis, we have plotted, in Figs. 8(a)–8(c) ($d_e = 1$) and Figs. 9(a)–9(c) ($d_e = 2$), $M(\ell)$ versus $\ell^{\delta'(2-\delta')}$, in a semilogarithmic fashion. The relative distance exponents δ' are 0.5, 1.25, and 1.75 in both cases. The lattice sizes are the same as in Figs. 4 and 5. For $\delta' = 0.5$ where the spatial constraints are irrelevant, we find $\log_{10} M \sim \ell$, in agreement with (10). In the intermediate δ regime $1 \leqslant \delta' < 2$ we find that $\log_{10} M \sim \ell^\alpha$, with $\alpha = 0.93$ ($\delta' = 1.25$) and 0.43 ($\delta' = 1.75$), also in agreement with (10). Accordingly, in the intermediate δ regime, $M(\ell)$ scales with the topological distance ℓ as a stretched exponential which serves as a "bridge" between the exponential behavior for $\delta < d_e$ and the anticipated power-law behavior for δ well above $2d_e$.

Now the question arises how the power law in Eq. (5) that describes the scaling of M with r and the stretched exponential in Eq. (10) that describes the scaling of M with ℓ can be simultaneously satisfied. The only way to fulfill both equations is that also $r(\ell)$ is a stretched exponential with the same α in the intermediate regime, i.e.,

$$r(\ell) \sim e^{B\ell^{\delta'(2-\delta')}}, \quad 1 \leqslant \delta' < 2, \tag{11}$$

and the ratio between the prefactors A and B should yield the dimension of the network. This is since $M(\ell) \sim e^{A\ell^{\delta'(2-\delta')}} = (e^{B\ell^{\delta'(2-\delta')}})^{A/B} \sim r^d$. Figures 8(e), 8(f), 9(e), and 9(f) support the assumption (11). The prefactor B is obtained from the slopes of the straight lines in the figures and indeed the values of A/B are found to be identical to the values of the dimensions we obtained in the previous section. For δ below d_e [see

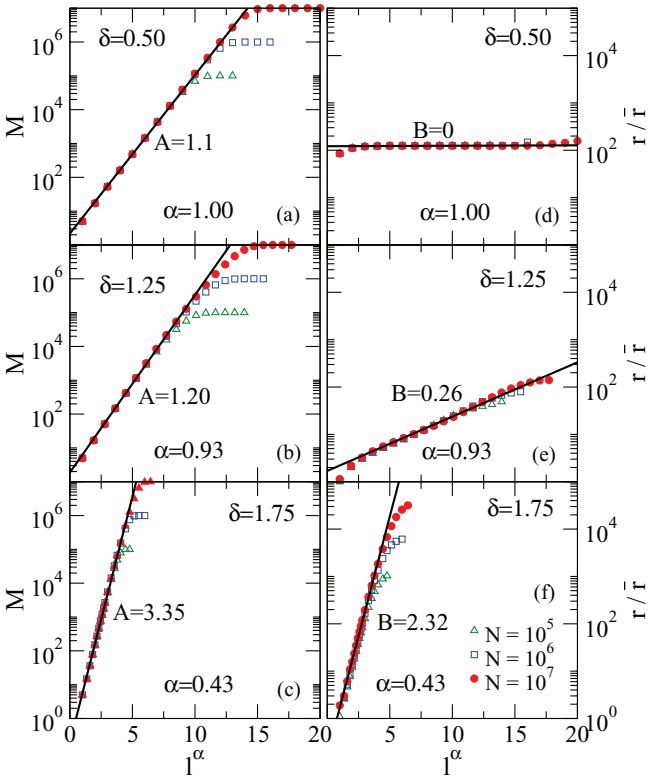

FIG. 8. (Color online) The mass M (left column) and the relative distance $r/\bar{r}$ (right column) as function of ℓ^{α} [ℓ is the topological distance and $\alpha = \delta'(2-\delta')$] for ER networks embedded in linear chains with $k = 4$, for the system sizes $N = 10^5$, 10^6, and 10^7 with $\delta = 0.5$, 1.25, and 1.75. The straight lines are best fits to the data with slopes A and B, respectively.

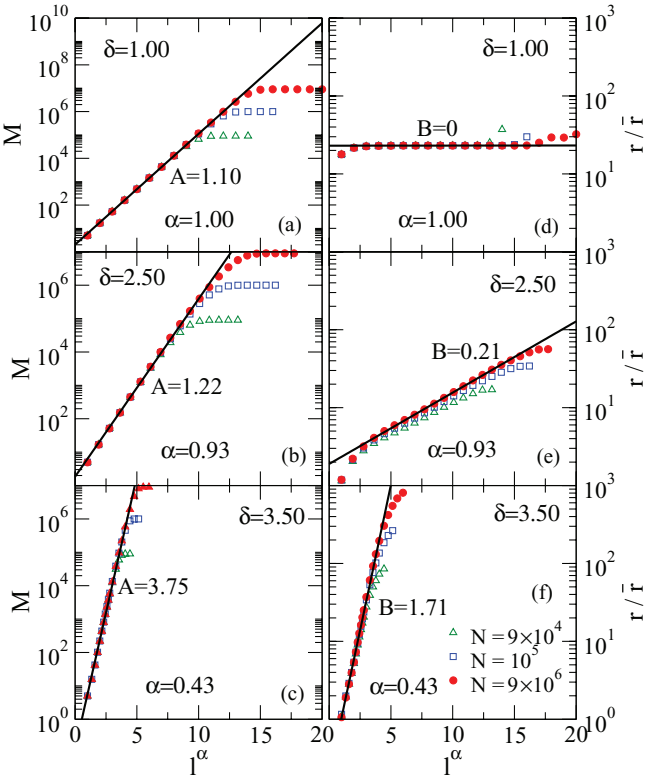

FIG. 9. (Color online) The same as Fig. 8, but for ER networks embedded in a square lattice, the system sizes are $N = 9 \times 10^4$, 10^6, and 9×10^6 with $\delta = 1.0$, 2.5, and 3.5.

Figs. 8(d) and 9(d)], r is independent of ℓ and $M \sim e^{A\ell}$ [see Figs. 8(a) and 9(a)].

For $\delta \geqslant 2d_e$, we expect that $M(\ell)$ and $r(\ell)$ follow power laws, such that we can determine, from a double logarithmic plot, the chemical dimension d_ℓ and the dimension of the shortest path, $d_{\min}$. Figures 10 and 11 show that this is the case. But surprisingly, for $\delta \geqslant 2d_e$ (but close to $2d_e$), the values of $d_{\min}$ and d_ℓ do not agree with the values for the corresponding regular lattices. For $\delta = 2d_e$, we obtain $d_\ell \simeq 3.02$ in $d_e = 1$ and $d_\ell \simeq 3.67$ in $d_e = 2$, significantly higher than the corresponding values $d_\ell = 1$ and $d_\ell = 2$ in regular lattices. Furthermore, the dimension of the shortest path $d_{\min}$ is considerably smaller than in regular lattices ($d_{\min} = 1$), $d_{\min} = 1/2.65 = 0.38$ in $d_e = 1$ and $d_{\min} = 1/1.80 = 0.56$ in $d_e = 2$. Since $M \sim \ell^{d_\ell} \sim r^{d_{\min} d_\ell}$, the dimension d of the network for $\delta \geqslant 2d_e$ is simply $d = d_{\min} d_\ell$, which yields $d \simeq 1.14$ in $d_e = 1$ and $d \simeq 2.04$ in $d_e = 2$, in agreement with our results of Figs. 4–7. For δ above $2d_e$ we expect that d_ℓ and $d_{\min}$ accept the values of the corresponding regular lattices. Figure 10 shows that this is indeed the case in $d_e = 1$, with a pronounced crossover behavior for $\delta = 2.25$ and 2.5. The crossover point decreases with increasing δ. In $d_e = 2$, in contrast, for $\delta = 2.25d_e$ and $2.5d_e$ the dimensions do not seem to reach their anticipated values $d_e = 2$ and $d_{\min} = 1$, even though $d \cong 2$ was obtained for both δ values. Figure 11 does not suggest that this is a finite-size effect since a bending down for larger system sizes cannot be seen similar to that in $d_e = 1$. However, we cannot exclude the possibility that at very large system sizes that right now cannot be analyzed with the current state-of-the-art computers, there will be a crossover towards the anticipated values of $d_\ell = 2$ and $d_{\min} = 1$.

VII. SUMMARY

In summary, we studied the effect of spatial constraints on complex networks where the length r of each link was taken from a power-law distribution, Eq. (1), characterized by the exponent δ. Spatial constraints are relevant in all networks where distance matters, such as the Internet, power grid networks, and transportation networks, as well as in cellular phone networks and collaboration networks [2,8,20,23–25]. Our results suggest that for δ below the embedding dimension d_e, the dimension of the network is infinite as in the case of networks that are not embedded in space (represented by $\delta = 0$). For δ between d_e and $2d_e$, the dimension decreases monotonically, from $d = \infty$ to $d = d_e$. Above $2d_e$, $d = d_e$. We also studied how the mass M and the Euclidean distance r scale with the topological distance ℓ. For δ below d_e, M increases exponentially with ℓ, while r does not depend on ℓ. For δ between d_e and $2d_e$, both the mass M and the Euclidean distance r increase with ℓ as a stretched exponential, with the same exponent α but different prefactors in the exponential. The ratio between these two prefactors yields the dimension of the embedded network. Exactly at $\delta = 2d_e$, the exponent α becomes zero and M and r scale with ℓ as power laws, defining

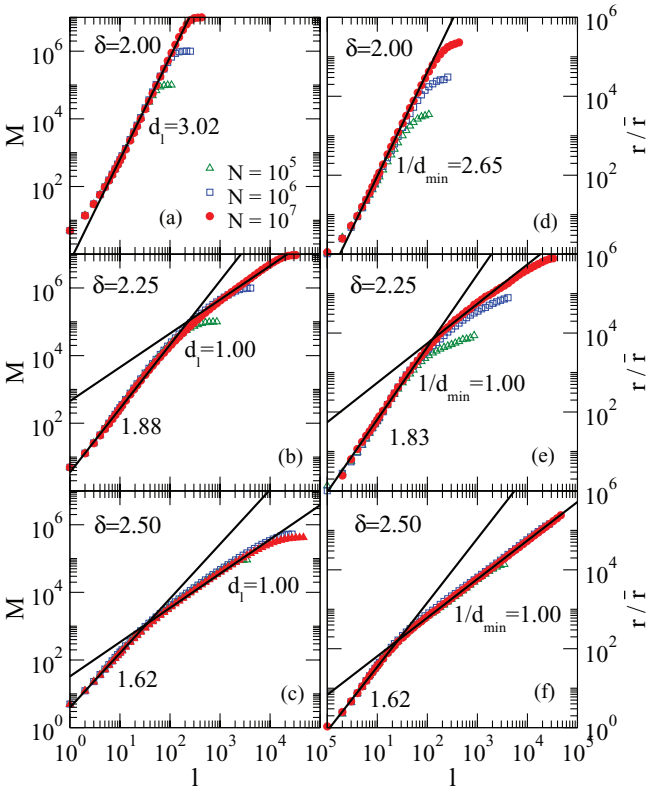

FIG. 10. (Color online) The mass M (left column) and the relative distance $r/\bar{r}$ (right column) as a function of the topological distance ℓ for ER networks embedded in linear chains with $k = 4$, for the system sizes $N = 10^5$, 10^6, and 10^7 with $\delta = 2.0$, 2.25, and 2.5. The straight lines are best fits to the data that yield the topological dimension d_l and the dimension of the shortest path $d_{\min}$. Note that the slopes below the crossover in (b), (c), (e), and (f) of M and r vs ℓ are the same. This yields $d = 1$ for all range of r as indeed seen in Fig. 4.

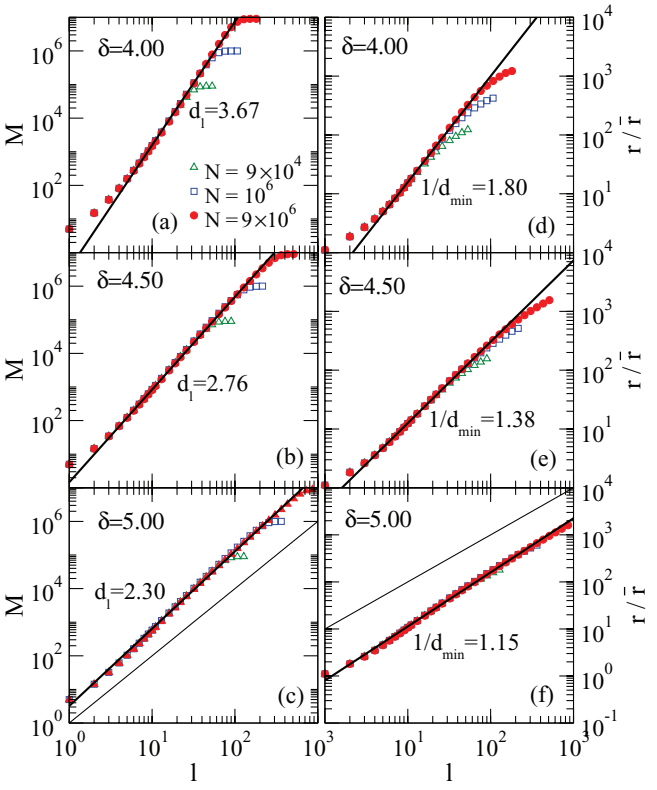

FIG. 11. (Color online) The same as Fig. 10, but for ER networks embedded in a square lattice. The system sizes are $N = 9 \times 10^4$, 10^6, and 9×10^6 with $\delta = 4.0$, 4.5, and 5.0. The lines in (c) and (f) demonstrate for comparison slopes 2 and 1, respectively.

the exponents d_ℓ and $d_{\min}$, respectively similar to fractal structures [39,44]. While the dimension d is equal to d_e, surprisingly d_ℓ and $d_{\min}$ do not have the values $d_\ell = d_e$ and $d_{\min} = 1$ that are expected for regular lattices. This effect seems to hold in $d_e = 2$ also for δ values somewhat greater than $2d_e$.

Our results have been obtained for a nearly δ-functional degree distribution, but we argue that they are valid for any narrow degree distribution, such as a Poissonian, Gaussian, or exponential degree distribution, since all those networks are expected to be in the same universality class. For power-law degree distributions (scale-free networks [29]), there may be differences for small values of δ, since it is known that nonembedded random graphs and scale-free networks are in different universality classes [45,46]. In the relevant intermediate δ regime ($d_e \leqslant \delta < 2d_e$), we cannot exclude the possibility that the dimensions do not depend on the degree distribution. Indications are from measurements of the dimension of the airline network and the Internet [32]. Both are scale-free networks, with δ close to 3 (airline network) and δ close to 2.6 (Internet). For the airline network, d is close to 3, while for the Internet, d is close to 4.5. These values are consistent with those obtained here for the ER networks, with the same δ values. We have assumed a power-law distribution, Eq. (1), for the link length. Other distributions are possible, for example an exponential distribution which holds for the power grid and ground transportation networks [20]. This case is equivalent to $\delta = \infty$, since we have a finite length scale and thus the dimension d of the network is expected to be the same as the dimension of the embedding space d_e.

A power-law distribution of Euclidean distances appears also in other physical systems where the present results may be relevant. For example, model systems where the interactions between particles decay as $r^{-\delta}$ have been studied extensively for many years; for recent reviews on the statistical physics and dynamical properties of these systems, see [47,48]. Magnetic models on lattices with long-range bonds whose lengths follow a power-law distribution have also been studied; see, e.g., [49]. In Levy flights and walks, the jump lengths follow a power-law distribution. For reviews see [41,50,51]. Finally, it has been found that a power-law distribution of link lengths with $\delta = d_e$ or $d_e + 1$ (depending on the type of transport) is optimal for navigation [14,34,52–54].

ACKNOWLEDGMENTS

A.B. and S.H. are grateful to the Deutsche Forschungsgemeinschaft for financial support. D.L. is supported by National Natural Science Foundation of China (Grant No. 61104144).

[1] R. Albert, H. Jeong, and A.-L. Barabási, Nature (London) **401**, 130 (1999).
[2] R. Albert and A.-L. Barabási, Rev. Mod. Phys. **74**, 47 (2002).
[3] D. J. Watts and S. H. Strogatz, Nature (London) **393**, 440 (1998).
[4] D. J. Watts, *Small Worlds* (Princeton University Press, Princeton, 1999).
[5] M. E. J. Newman, D. J. Watts, and S. H. Strogatz, Proc. Natl. Acad. Sci. U.S.A. **99**, 2566 (2002).
[6] R. Milo, S. Shen-Orr, S. Itzkovitz, N. Kashtan, D. Chklovskii, and U. Alon, Science **298**, 824 (2002).
[7] S. N. Dorogovtsev, *Evolution of Networks: From Biological Nets to the Internet and WWW* (Oxford University Press, Oxford, 2003).
[8] R. P. Satorras and A. Vespignani, *Evolution and Structure of the Internet: A Statistical Physics Approach* (Cambridge University Press, Cambridge, 2004).
[9] L. K. Gallos, R. Cohen, P. Argyrakis, A. Bunde, and S. Havlin, Phys. Rev. Lett. **94**, 188701 (2005).
[10] B. Bollobás, *Random Graphs* (Cambridge University Press, Cambridge, 2001).
[11] A. Barrat, M. Barthélmy, and A. Vespignani, *Dynamical Processes on Complex Networks* (Cambridge University Press, Cambridge, 2008).
[12] D. Brockmann, L. Hufnagel, and T. Geisel, Nature (London) **439**, 462 (2006).
[13] R. Cohen, K. Erez, D. ben-Avraham, and S. Havlin, Phys. Rev. Lett. **85**, 4626 (2000).
[14] Y. Hu, Y. Wang, D. Li, S. Havlin, and Z. Di, Phys. Rev. Lett. **106**, 108701 (2011).
[15] M. E. J. Newman, *Networks: An Introduction* (Oxford University Press, Oxford, 2010).
[16] G. Csanyi and B. Szendroi, Phys. Rev. E **70**, 016122 (2004).
[17] M. T. Gastner and M. E. J. Newman, Eur. Phys. J. B **49**, 247 (2006).
[18] R. Cohen and S. Havlin, *Complex Networks: Structure, Robustness, and Function* (Cambridge University Press, Cambridge, 2010).
[19] R. Cohen and S. Havlin, Phys. Rev. Lett. **90**, 058701 (2003).
[20] M. Barthélmy, Phys. Rep. **499**, 1 (2010).
[21] A. Barrat, M. Barthélmy, R. Pastor-Satorras, and A. Vespignani, Proc. Natl. Acad. Sci. U.S.A. **101**, 3747 (2004).
[22] G. Bianconi, P. Pin, and M. Marsili, Proc. Natl. Acad. Sci. U.S.A. **106**, 11433 (2009).
[23] H. Hua, S. Myers, V. Colizza, and A. Vespignani, Proc. Natl. Acad. Sci. U.S.A. **106**, 1318 (2009).
[24] D. Liben-Nowell, J. Novak, R. Kumar, P. Raghavan, and A. Tomkins, Proc. Natl. Acad. Sci. U.S.A. **102**, 11623 (2005).
[25] R. Lambiotte, V. D. Blondel, C. de Kerchove, E. Huens, C. Prieur, Z. Smoreda, and P. Van Dooren, Physica A **387**, 5317 (2008).
[26] H. Jeong, S. Mason, A.-L. Barabási, and Z. N. Oltvai, Nature (London) **411**, 41 (2001).
[27] P. Erdös and A. Rényi, Publ. Math. Debrecen **6**, 290 (1959).
[28] P. Erdös and A. Rényi, Publ. Math. Inst. Hung. Acad. Sci. **5**, 17 (1960).
[29] A.-L. Barabási and R. Albert, Science **286**, 509 (1999).
[30] K. Kosmidis, S. Havlin, and A. Bunde, Europhys. Lett. **82**, 48005 (2008).
[31] D. Li, G. Li, K. Kosmidis, E. H. Stanley, A. Bunde, and S. Havlin, Europhys. Lett. **93**, 68004 (2011).
[32] D. Li, K. Kosmidis, A. Bunde, and S. Havlin, Nat. Phys. **7**, 481 (2011).
[33] J. Goldberg and M. Levy, arXiv:0906.3202.
[34] J. M. Kleinberg, Nature (London) **406**, 845 (2000).
[35] A. F. Rozenfeld, R. Cohen, D. ben-Avraham, and S. Havlin, Phys. Rev. Lett. **89**, 218701 (2002).
[36] S. S. Manna and P. Sen, Phys. Rev. E **66**, 066114 (2002).
[37] C. P. Warren, L. M. Sander, and I. M. Sokolov, Phys. Rev. E **66**, 056105 (2002).
[38] R. Xulvi-Brunet and I. M. Sokolov, Phys. Rev. E **66**, 026118 (2002).
[39] A. Bunde and S. Havlin (eds.), *Fractals and Disordered Systems* (Springer, Berlin, 1991).
[40] G. H. Weiss, *Aspects and Applications of the Random Walk* (North Holland Press, Amsterdam, 1994).
[41] J. Klafter and I. M. Sokolov, *First Steps in Random Walks* (Oxford University Press, Oxford, 2011).
[42] D. Ben-Avraham and S. Havlin, *Diffusion and Reactions in Fractals and Disordered Systems* (Cambridge University Press, Cambridge, 2010).
[43] S. Alexander and R. Orbach, J. Phys. Lett. **43**, 625 (1982).
[44] S. Havlin and D. Ben-Avraham, Adv. Phys. **51**, 187 (2002); **36**, 695 (1987).
[45] R. Cohen, D. ben-Avraham, and S. Havlin, Phys. Rev. E **66**, 036113 (2002).
[46] S. N. Dorogovtsev, A. V. Goltsev, and J. F. F. Mendes, Rev. Mod. Phys. **80**, 1275 (2008).
[47] D. Mukamel, arXiv:0811.3120.
[48] A. Campa, T. Dauxois, and S. Ruffo, Phys. Rep. **480**, 57 (2009).
[49] Y. F. Chang, L. Sun, and X. Cai, Phys. Rep. **76**, 021101 (2007).
[50] J. Klafter, M. F. Shlesinger, and G. Zumofen, Phys. Today **49**(2), 33 (1996).
[51] R. Metzler and J. Klafter, Phys. Rep. **339**, 1 (2000).
[52] G. M. Viswanathan, S. V. Buldyrev, S. Havlin, M. G. E. da Luz, E. P. Raposo, and E. H. Stanley, Nature (London) **401**, 911 (1999).
[53] G. Li, S. D. S. Reis, A. A. Moreira, S. Havlin, H. E. Stanley, and J. S. Andrade, Phys. Rev. Lett. **104**, 018701 (2010).
[54] M. R. Roberson and D. ben-Avraham, Phys. Rev. E **74**, 017101 (2006).